Proceedings of CREEP8
Eighth International Conference on Creep and Fatigue at Elevated Temperatures
July 22-26, 2007, San Antonio, Texas

CREEP2007-26397

CREEP-FATIGUE DAMAGE AND CRACK INITIATION FOR A MOD 9CR-1MO STRUCTURE WITH WELDMENTS

Hyeong-Yeon Lee , Se-Hwan Lee, Jong-Bum Kim, Jae-Han Lee
Korea Atomic Energy Research Institute
150 Dukjin-dong, Yusong-gu, Daejeon 305-353, Korea

ABSTRACT

A structural test and evaluation on creep-fatigue damage, and creep-fatigue crack initiation have been carried out for a Mod. 9Cr-1Mo steel structural specimen with weldments. The conservatisms of the design codes of ASME Section III subsection and NH and RCC-MR codes were quantified at the welded joints of Mod.9Cr-1Mo steel and 316L stainless steel with the observed images from the structural test. In creep damage evaluation using the RCC-MR code, isochronous curve has been used rather than directly using the creep law as the RCC-MR specifies. A y-shaped steel specimen of a diameter 500mm, height 440mm and thickness 6.35mm is subjected to creep-fatigue loads with two hours of a hold time at 600°C and a primary nominal stress of 30MPa. The defect assessment procedures of RCC-MR A16 guide do not provide a procedure for Mod.9Cr-1Mo steel yet. In this study application of σ_d method for the assessment of creep-fatigue crack initiation has been examined for a Mod. 9Cr-1Mo steel structure.

INTRODUCTION

Assessment of the integrity of a structure operating at high temperature under creep-fatigue loading conditions is of key importance for the safe and reliable operation of nuclear and conventional power plants. Modified 9Cr-1Mo steel (ASME Grade 91) has been widely used with relatively short period of history for a high temperature structure such as a steam generator, intermediate heat exchanger and secondary piping of a liquid metal reactor [1], and fossil power plants. Grade 91 has economic competitiveness, relatively low thermal expansion coefficient, high thermal conductivity, high mechanical strength and good resistance against irradiation swelling. However, concern of cracking in heat-affected zone and subsequent failure, commonly known as Type IV cracking, exists at the welded joints for long term services [2,3,4]

The current versions of high temperature design codes, ASME Section III Subsection NH[5] or RCC-MR[6] provide design guidelines for Grade 91 component but do not provide complete guideline for Grade 91 welded assemblies yet. The design procedure for Grade 91 has been first implemented in 2004 edition of ASME-NH, and they don't provide full fatigue data and creep rupture data, while the coefficients of weld characteristics are not completely provided in RCC-MR. It is reported that the linear damage summation rule for the creep-fatigue damage originally developed for austenitic stainless steel could give poor results for Grade 91 and the evaluation results could be overly conservative [7,8]. The damage envelopes in ASME-NH and RCC-MR for creep-fatigue of Grade 91 are significantly different. The differences have yet to be explained by the scatter in the data, the variation of the heats, the material softening, to see whether a creep-fatigue damage envelope is procedure dependent or not [8]. The researches on a creep-fatigue damage and creep-fatigue crack behaviour have been carried out for austenitic stainless steel structure with weldments [9,10]. The current A16 guide does not provide an assessment guide on the creep-fatigue crack initiation and propagation for Grade 91 structure. In this study, assessment on creep-fatigue crack initiation by using σ_d approach has been carried out for Grade 91 structure based on the '*d*' value of '*d*=36μm' [11].

The structural test model representing IHX(Intermediate Heat eXchanger) support structure of a liquid metal reactor [1] has dissimilar metal welds(Mod. 9Cr-1Mo vs. 316L) as well as similar metal welds(between Grade 91 and Grade 91, and between 316L and 316L). The comparison of the creep-fatigue damage by test and evaluation according to ASME-NH and RCC-MR code for the base and weld metals has been carried out.

CREEP-FATIGUE STRUCTURAL TEST

Specimen details

A structural specimen shown in Fig. 1 and Fig. 2, which represents an IHX support structure, has the dimensions of a 500mm diameter, a 440mm height and a 6.35mm thickness. The specimen is made of Grade 91 and 316L stainless steel.

The schematic diagram of the test facility and y-shaped specimen with five welded joints in the outer shell is shown in Fig. 1. The parts of interest in this specimen are outer shell and y-piece bent part of the specimen. The Fig. 1 shows that structural specimen installed inside the induction coils. The creep-fatigue test facility shown in Fig. 1 is composed of a hydraulic actuator of a 1MN capacity and a high frequency induction heater with a capacity of 50kW. The induction coil set was fabricated with a number of trial and errors by changing the gaps between the coils to minimize the temperature difference in axial direction over the outer shell.

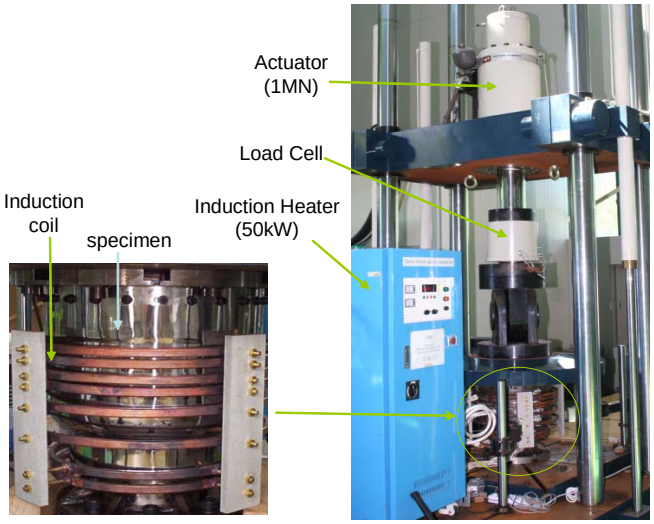

Fig. 1 Structural specimen and creep-fatigue test facility

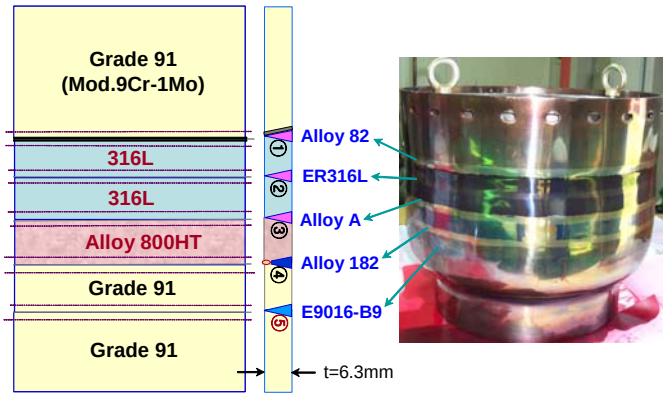

Fig. 2 Composition of the materials in the outer shell of the specimen

Three materials of Grade 91, Alloy 800HT and 316L stainless steel were used in outer shell of the structural specimen as shown in Fig. 2.

Table 1. Comparison of mechanical strengths

(at room temperature, unit : MPa)

	YS (ASME-NH)	YS (as-received)	UTS (as- received)
Grade 91	413.6	604	742
Alloy 800HT	172.4	255	450
316L	207.0	275	590

The mechanical properties of as-received material and ASME-NH are compared in Table 1, which shows that the as-received material has higher strength with some cold working than code properties. Alloy 800HT is very similar to Alloy 800H (ASME-NH material) except slight difference in the chemical compositions of Aluminum and Titanium.

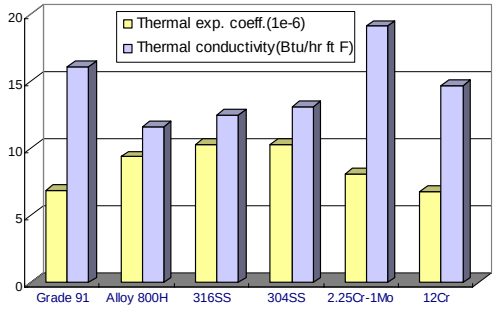

Fig. 3 Comparison of thermal properties [5,12] at 538°C

Grade 91 has relatively low thermal expansion coefficient and high thermal conductivity as shown in Fig. 3. The mechanical properties of Grade 91 shows that it has high yield strength(σ_y) while hardening up to UTS(σ_u) is small when compared with other materials as shown in Fig. 4. The design stress intensity [5], σ_m of Grade 91 is larger than the other five materials as shown in Fig. 4.

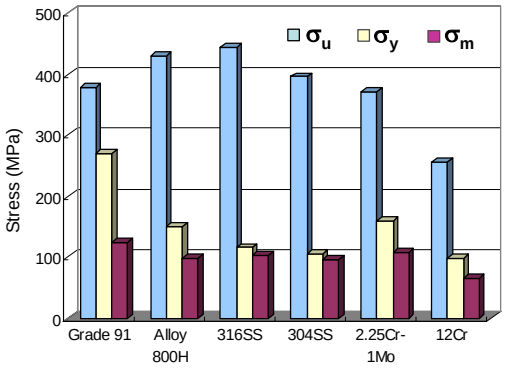

Fig. 4 Comparison of mechanical properties [5,12] at 538°C

Weld Details

Two methods of dissimilar metal welds between Grade 91 and austenitic 316L stainless steel were applied. As shown in Fig. 5, in the welding between Grade 91 and 316L, the upper part of the outer shell employed a buttering weld using filler metal of Alloy 82 (Inconel 82) while the lower part applied a trimetallic transition welding by inserting Alloy 800HT which has in-between thermal expansion coefficients of 316L and Grade 91.

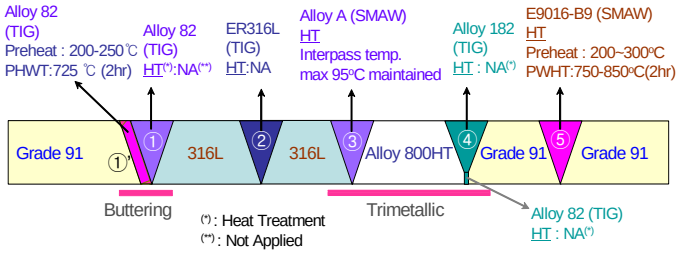

Fig. 5 Weld details and heat treatments

The details of filler metals used for the circumferential welding and heat treatment are shown in Fig. 5. The filler metal at the weld line of 1 to 5 in Fig. 2 is Alloy 82, ER316L, Alloy A(ENiCrFe-2), Alloy 182 (Inconel 182) and E9016-B9(Mod.9Cr-1Mo), respectively. In the specimen, there are three locations of dissimilar welds at weld number 1(Grade 91-316L), weld No. 3 (316L-Alloy 8HT) and weld No. 4(Alloy 800HT-Grade91). There are two locations of similar metal welds at weld number 2(316L-316L) and weld No. 5(Grade91-Grade91).

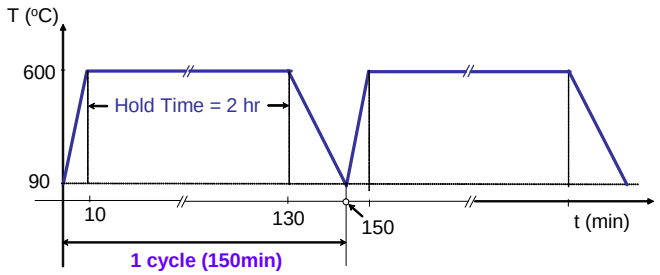

Fig. 6. Thermal load conditions with two hours of a hold time

Load conditions

The specimen was subject to a creep-fatigue load as shown in Fig. 6. The specimen was heated up to 600°C and the hold time at 600°C was two hours. It took about 10 minutes to reach 600°C from 90°C and 20 minutes to cool down to 90°C. So, one cycle is about 150 minutes including two hours of a tensile hold time as shown in Fig. 6. Mechanical load of 30 tons has been applied in the axial direction of the specimen and the axial nominal stress at the outer shell was 30.0MPa. Totally 200 cycles (hold time=400 hours) of creep-fatigue load has been carried out.

The target temperature of the specimen was 600°C but the temperature distribution along the axial direction is not uniform due to differences in heating characteristics under induction heating of the material of Grade 91, Alloy 800HT and 316L. The measured temperature data of the specimen was partly heated over 600°C while the lowest is about 520°C as shown in Fig. 7. In actual observation, the maximum temperature difference along the axial direction over the region of interest was measured to be about 100°C. The figure shows the temperature histories at the six locations of the specimen. These temperature profiles were used as thermal load input in creep-fatigue damage evaluation.

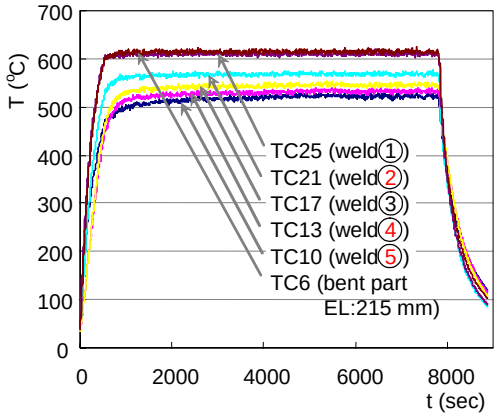

Fig. 7. Temperature data measured at six locations of specimen

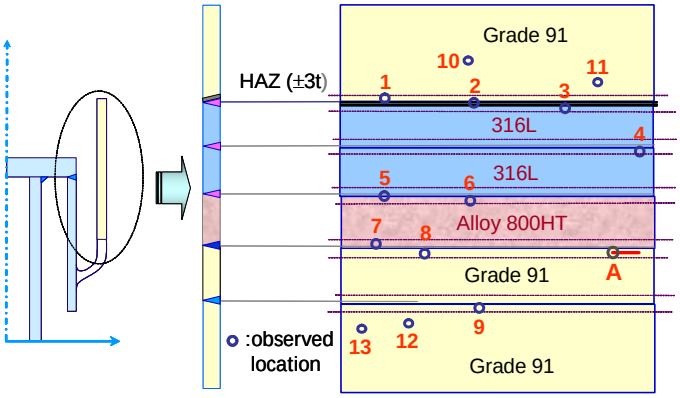

Fig. 8 Observed locations of the specimen using optical microscope

Observation of creep-fatigue damage

A portable optical microscope was used to observe the

creep-fatigue damage of the test specimen with the interval of 50 cycles (hold time=100 hours) intermittently up to 200 cycles. Thirteen locations of the specimen were selected as shown in Fig. 8. Those locations were ground, polished, and etched according to the standard procedure [13]. Final step for the surface preparation is etching and the composition of etchant is 2.5% picric acid, 2.5% HCl and 95% ethyl alcohol for Grade 91 (both at base and weld metal), 97ml HCl, 2ml H_2SO_4 and 1ml HNO_3 for Alloy 800HT, and 8% HNO_3, 54% HCl, and 38% H_2O for 316L stainless steel.

The observed images at each material of the specimen will show the degree of the actual damage and they will be compared with evaluation results of the design codes of ASME-NH and RCC-MR.

EVALUATION OF CREEP-FATIGUE DAMAGE AND CRACK INITIATION

Finite element modeling

The 2D ABAQUS[14] axisymmetric finite element model shown in Fig. 9(a) was used for the evaluation of creep-fatigue damage and 3D model of Fig. 9(b) was used for the evaluation of creep-fatigue crack initiation. Thermal loads of Fig. 6 measured by using 28 thermocouples and a tensile mechanical load of 30 tons which results in a nominal stress of 30.0MPa at the outer shell were applied. The bottom surface was fixed as a boundary condition as shown in Fig. 9(a). There are five welded joints as shown in Fig. 8. Creep-fatigue damage was evaluated at the three selected welded joints of weld No. 2, 4 and 5 in Fig. 9(a). The FE results at these locations were used for creep-fatigue damage evaluation.

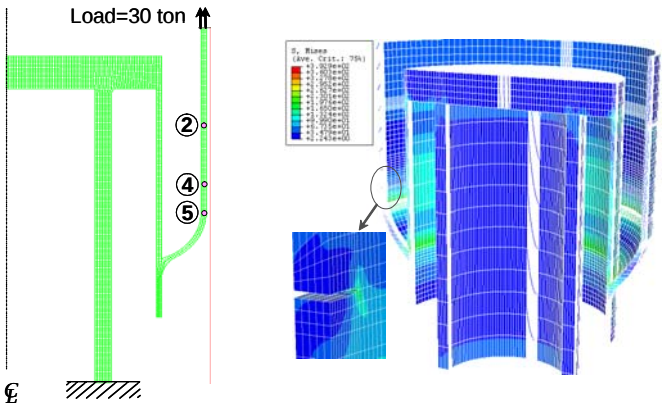

(a) axisymmetric model (b) 3D model

Fig. 9. Finite element model

Creep-fatigue damage

The evaluation of creep-fatigue damage was carried out for a defect free part while assessment on creep-fatigue crack initiation was carried out for a part with a defect. The evaluation of creep-fatigue damage has been carried out according to the ASME-NH and RCC-MR code. The linear damage summation rule is used for both codes in determining a creep-fatigue damage, but the calculation procedures of the two design codes are quite different especially on the following points.

In determining a total strain range, ASME-NH adopts a strain based approach and determines the total strain by using the equivalent strains while RCC-MR adopts similar strains composed of a four terms based approach but uses stress intensities to determine four components of the strains.

ASME-NH uses isochronous curves while RCC-MR uses stress-strain cyclic curves and a separate creep law is directly used to determine creep damage. The safety factor for a creep evaluation in RCC-MR uses a unique value of 0.9 for all materials while in ASME-NH it is 0.87 for Grade 91 and 0.67 for the other materials listed in ASME-NH. The creep-fatigue damage envelopes for ASME-NH are material specific while those for RCC-MR are the same for all Code materials as shown in Fig. 10.

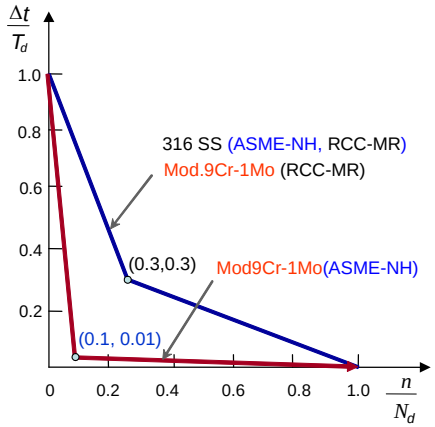

Fig. 10. Creep-fatigue damage envelope for the ASME-NH and RCC-MR

The evaluation procedure for a welded joint in ASME-NH and RCC-MR uses different methods. In ASME-NH, in the vicinity of a weld (defined by ±3 times the thickness to either side of the weld centre line), the N_d value shall be one-half the value permitted for the parent material while T_d value is determined from stress-to-rupture values by weld strength reduction factors of the base metal [5].

In RCC-MR, the allowable stress-to-rupture values for the welded joint are replaced by J_r(creep strength reduction factor) times the stress-to-rupture values for the base metal. The total stress range for weldment is determined by a stress range multiplied by a fatigue strength reduction factor f [6]. And the fatigue curve of the welded joint is determined by dividing the ordinates of the reference curve for the base metal by the coefficient of the weld fatigue characteristics, J_f. The present 2002 edition of the RCC-MR code [6] provides the weld factors only for limited cases.

The linear damage summation rule for creep-fatigue damage was developed by Severud [15]. Its concept is originally based on the cavity growth of austenitic stainless steel and the creep-fatigue damage is determined from the linear summation of fatigue damage and creep damage. Since there is interaction between creep and fatigue, the damage envelop is bilinear shape with interaction point rather than linear shape. The creep-fatigue damage envelopes for the two materials of Grade 91 and 316 SS are provided as material specific as shown in Fig. 10. It should be noted that the intersection points of the envelopes in current design codes are material specific. Therefore, strictly speaking this rule is not appropriate for Grade 91 and Alloy 800H because the damage modes especially for creep are different from austenitic stainless steel. The observation results from the test for Grade 91, Alloy 800H and 316L stainless steel could be useful in quantifying the conservatism of the design codes.

In DOE-ASME Generation IV materials tasks, two tasks out of the currently initiated five tasks are related to the improvement on the creep-fatigue of Grade 91 [8]. As shown in Fig. 10, the damage envelopes for the creep-fatigue for Grade 91 are significantly different in the ASME-NH and RCC-MR codes. It should be noted that the intersection point of the bilinear envelope for Grade 91 is (0.1, 0.01) in ASME-NH while it is (0.3, 0.3) in RCC-MR. The creep-fatigue behavior of Grade 91 is known to be weaker at a compressive hold than at a tensile hold [16]. Therefore, a creep-fatigue damage rule for Grade 91 should address these characteristics.

As an alternative rule for creep-fatigue damage of Grade 91, researches on ductility exhaustion and modified ductility exhaustion method were carried out [2].

Creep-fatigue crack initiation

In the French RCC-MR code[6], the geometrical discontinuities are assimilated with cracks for a creep-fatigue estimation based on an elastic analysis. The A16 guide [17] which is a technical appendix of the RCC-MR can be employed for an evaluation of the creep-fatigue crack initiation for a component with geometrical discontinuities. The creep-fatigue crack initiation of the A16 procedure is based on the σ_d method. The principal of this procedure is to determine a stress and a strain at a characteristic distance '*d*' ahead of the crack tip and to compare them with the material fatigue curve and the creep strength data [5,6,12]. The distance '*d*' is specified as '50μm' for austenitic stainless steels [17], which means crack initiation of 50μm for the material occurs if creep-fatigue damage according to A16 procedure reaches a critical value.

The distance '*d*' for Grade 91 is not provided in A16 yet and is proposed as '36μm' [11]. If creep-fatigue damage for Grade 91 according to A16 procedure reaches a critical value, it means that crack initiation with the amount of 100μm occurs based on the experimental findings. Using electrical potential curve, initiation was defined as an existing crack of 0.1mm which corresponds to a variation of electric potential drop of 8mV [11].

Evaluation of fatigue crack incubation usage factor is obtained by the ratio of the specified number of cycles to the number of the cycles prior to a fatigue initiation. Evaluation of the creep crack incubation usage factor is obtained by the ratio of the specified duration of the hold time '*t*' to the time prior to a creep initiation '*T*' determined from the usual creep rupture property.

In this study, the '*d*' value of 36μm was used for Grade 91 material part. The elastically calculated Rankine equivalent stress (the largest principal stress) at distance '*d*' ahead of the notch tip was determined by using an elastically calculated stress and the stress was used to determine fatigue crack incubation and creep crack incubation according to A16 procedure.

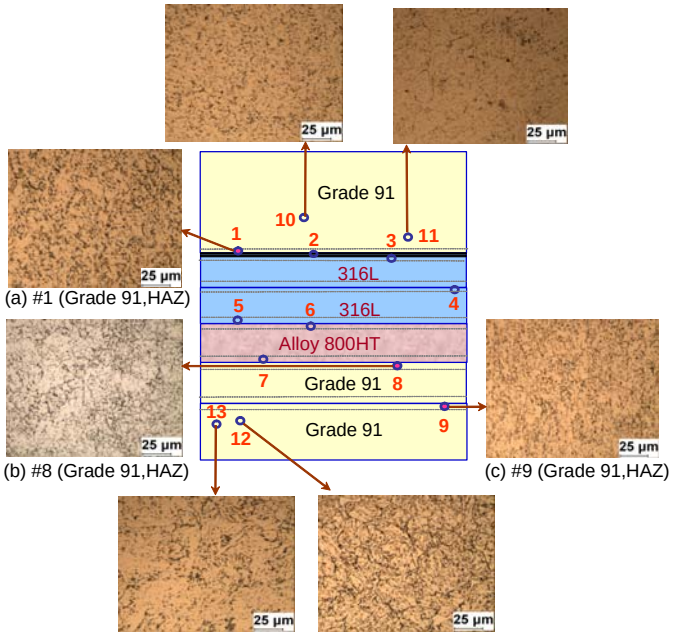

Fig. 11 Observed images for Mod.9Cr-1Mo steel at #1, #7 and #9 (after 200 cycles and 400 hours of hold time)

RESULTS

Test results

The results of creep-fatigue test are damage observed on the surface whereas the results of thermal ratcheting are deformation [18-21]. The images of the specimen surfaces have been observed with optical microscope in non-destructive way at every 50 cycles interval up to 200 cycles (hold time = 400 hours). The thirteen points of interest in the specimen were observed and analyzed.

For Grade 91 material, observations at base and HAZ were carried out. The image of Fig. 11 at point #1 (in Fig. 8) (HAZ, dissimilar metal weld of buttering) shows that there is no

visible damage up to 200 cycles (HT=400 hours). Another image at point #8 (HAZ, dissimilar transition weld) shows that no damage was observable either as shown in Fig. 11. For the welded joint of point # 9, which is similar metal welds (Grade 91 and Grade 91), no damage was observed. Up to 200 cycles of creep-fatigue load, it was observed that there is no significant difference between dissimilar welds and similar welds.

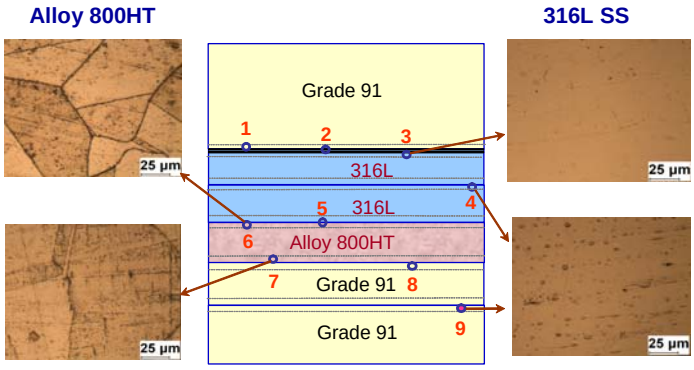

Fig. 12 Observed images at upper and lower part of Alloy 800HT and 316L

For Alloy 800HT at the point of #6 and #7 (both HAZ), no visible damage were observed as shown in Fig. 12. For 316L stainless steel at the point of #3 and #4 (both HAZ), slight damage on the surface was observed on the surface at point 4 as shown in Fig. 12.

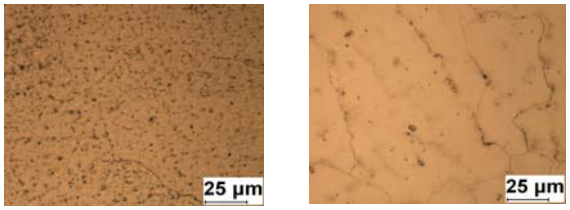

#2 (Alloy 82) #5 (Alloy A)

Fig. 13 Observed images at filler metals

For the filler metals of Inconel, observations were carried out for the point #2 (Alloy 82) and point #5 (Alloy A). Fig. 13 shows that the damage at these filler metals of Inconel material is most serious in the specimen. Especially the filler metal of point #5 was severe.

The image at the defect '*A*' of HAZ of Grade 91 at the notch of in Fig. 14 shows that no distinct damage was observed at the heat affect zone of '*A*'.

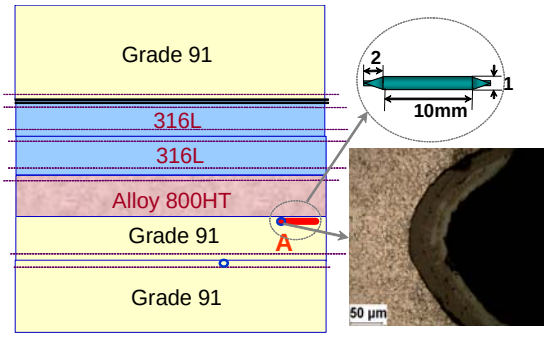

Fig. 14 Observed images at filler metals

As a whole, there were no visible damage for the material of Grade 91 and Alloy 800HT at defect free parts. However, there was slight damage at HAZ of 316L and damage was observed to be larger on the filler metal of point #2 and #5.

Evaluation results according to ASME-NH

The elastic-plastic strain range ($\Delta\varepsilon_{el+pl}$), creep strain range ($\Delta\varepsilon_{cr}$) and total strain range ($\Delta\varepsilon_t$) for the three welded joints (shown in Fig. 9(a)) were calculated according to ASME-NH and RCC-MR. The weak parts in a structure with weldments are usually HAZ[2-4], and the critical three locations in terms of a creep-fatigue damage were HAZ. Type IV cracking may occur at locations #4 or #5 of the Grade 91 joint when the accumulated damage reaches a critical value.

The evaluation results of creep-fatigue damage for the three locations shown in Fig. 9(a) are calculated as in Eq. (1) to (3) in order.

$$\frac{n}{65165} + \frac{\Delta t}{5171} \le D \qquad (1)$$

$$\frac{n}{>10^8} + \frac{\Delta t}{201} \le D \qquad (2)$$

$$\frac{n}{0.6} + \frac{\Delta t}{T_d \to 0} \le D \qquad (3)$$

When 200 cycles of creep-fatigue load was applied, the evaluation results show that Grade 91 locations with the envelope intersection point (0.1, 0.01) would fail. The welded joint of #2 will be damaged but not fail under the present creep-fatigue load.

When compared with the observed images of Figs. 11 and 14 which showed no visible damage, ASME-NH code was shown to be overly conservative for the present Grade 91 specimen.

Evaluation results according to RCC-MR

The elastic-plastic strains, creep strains and total strain ranges were calculated according to the RCC-MR code. The

evaluation results at the three welded joints of 2,4 and 5 of Fig. 9 according to RCC-MR were determined as follows;

$$\frac{n}{>10^6} + \frac{\Delta t}{94664} \le D \quad (4)$$

$$\frac{n}{9662485} + \frac{\Delta t}{21} \le D \quad (5)$$

$$\frac{n}{118} + \frac{\Delta t}{11} \le D \quad (6)$$

RCC-MR employs material specific creep laws and cyclic stress-strain curves to determine the creep damage while ASME-NH uses isochronous curve data although both codes employ Robinson's time fraction rule. The creep law in RCC-MR for Grade 91 and 316L is the Bailey-Norton creep law [22]. When comparing the two results for the creep rupture times between the two codes it is shown that the creep rupture times by RCC-MR are larger than those by ASME-NH at weld #2(similar weld of 316L) and #5(similar weld of Grade 91) while RCC-MR is smaller than ASME-NH at weld #4(dissimilar weld of Grade 91 and Alloy 800H).

It should be noted that creep damage in RCC-MR depends on the material specific creep law provided in A3 [22] of the RCC-MR. It should also be noted that since the allowable area in the creep-fatigue damage envelopes of ASME-NH is considerably smaller than those of RCC-MR for Grade 91, its acceptability should be judged with the material specific damage envelope.

When t=400 is applied, the RCC-MR results show that all locations except weld #2(Eq. 2) will fail because the intersection point of all materials in RCC-MR is (0.3,0.3).

From the above analysis, it seems to be necessary to complement data in ASME-NH on extending stress-to-rupture data to higher stress values and preparing the stress rupture factors for Grade 91 welded joint as functions of hold time so that more reliable result on creep damage at the welded joint can be obtained. In RCC-MR creep-fatigue evaluation procedure, weld strength reduction factors for Alloy 800H and Grade 91 should be complemented. In addition, the creep-fatigue evaluation procedures of ASME-NH and RCC-MR should be improved based on validation tests as well as evaluation results especially for Grade 91.

The creep-fatigue crack initiation (incubation) for the defect '*A*' in Fig. 8 was calculated as follows;

$$\frac{n}{49.5} + \frac{\Delta t}{6.6} \le D \quad (7)$$

The Eq. (7) shows that creep crack incubation under less than 6.6 hours of hold time would cause crack initiation at the notch of '*A*' in Fig. 8. The σ_d value determined at the notch '*A*' according to the A16 guide was 319.04 (MPa). Since the observed image at that location shows no visible damage up to 400 hours of, it means that the current assessment result according to A16 procedure is very conservative for the present model and loading condition. It should be noted that in Eq. (7) the factor of 1.5 was divided to the total strain range and factor of 1.0 (not 0.9) was divided to creep to determine more realistic damage.

The evaluation results for creep-fatigue damage and creep-fatigue crack initiation on the present structural model show that both ASME-NH and RCC-MR codes (RB-3200 and A16 guide) were overly conservative for Grade 91 part when compared with the observed images from the structural test.

CONCLUSIONS

A creep-fatigue test and evaluation were carried out for a structural specimen representing IHX support structure made of Grade 91(Mod. 9Cr-1Mo steel) and 316L stainless steel. In present structural test, totally 200 cycles (hold time=400 hours) was applied.

Comparison studies were conducted between the results of evaluation and structural test for a Grade 91 test specimen. First, the evaluations on creep-fatigue damage according to the ASME-NH and RCC-MR were carried out and the evaluation results were compared with those of the test. Comparisons between the two codes were also conducted. Second, evaluation of creep-fatigue crack initiation according to the A16 guide of RCC-MR for a defect at Grade 91 was carried out and the result was compared with the observed image.

When the evaluation results of the creep-fatigue damage according to the two design codes are compared, the ASME-NH was shown to be more conservative in terms of fatigue and creep damage. The allowable region in creep-fatigue damage envelope is far smaller in ASME-NH with the intersection point of (0.1,0.01) than in RCC-MR with the point of (0.3,0.3) for Grade 91, which made the ASME-NH overly conservative for the present Grade 91 structure.

The creep-fatigue damage in RCC-MR was calculated by using the material specific creep law provided in A3 of RCC-MR. In present study, the creep damage was evaluated by using isochronous curves rather than following the RCC-MR procedure because it was shown that the calculation results using directly the creep law gave inappropriate value for Grade 91. Although there are slight differences in material properties between ASME-NH and RCC-MR, the impact of the differences on the creep damage were negligible. The evaluation of creep damage according to RCC-MR route in combination with isochronous curve gave more reasonable value for Grade 91.

The observed images from the present structural test showed that both ASME-NH and RCC-MR codes for creep-fatigue damage were very conservative for Grade 91. When the creep-fatigue damage evaluation results of Eq.(1) to Eq. (6) were compared, the ASME-NH was shown to be more conservative than the RCC-MR for the present problem. The actual observation results showed that no damage were visible for those welded joints.

Assessment on creep-fatigue crack initiation for Grade 91 has been carried out according to the σ_d approach of the A16 procedure. Since A16 does not provide the guide for Grade 91, the '*d*' value of 36μm[11] was used. The assessment result was compared with the observed image from Grade 91 structural test. The observed image showed that the assessment result was very conservative for the present structural test.

ACKNOWDEMENTS

This study was supported by the Korean Ministry of Science & Technology through its National Nuclear Technology Program.

REFERENCES

[1] D-H Hahn et al., KALIMER-600 Preliminary Conceptual Design Report, KAERI/TR-2784, Korea Atomic Energy Research Institute, Daejeon; 2004.

[2] Y Takhashi, Study on Type-IV Damage Prevention in High-Temperature Welded Structures of Next-Generation Reactor Plants, Part I Fatigue and Creep-Fatigue Behaviour of Welded Joints of Modified 9Cr-1Mo Steel, PVP2006-ICPVT-11-93081, July 23-27, Vancouver, Canada; 2006.

[3] S Brett, D Oates, C Johnston, In-Service Type IV Cracking in a Modified 9Cr (Grade 91) Header, ECCC Creep Conference, London : 563-672, September 2005.

[4] M Tabuchi, Y Takhashi, Evaluation of creep streingth reduction factors for welded joints of modified 9Cr-1Mo steel (P91), PVP2006-ICPVT-11-93350, July 23-27, Vancouver, Canada; 2006.

[5] ASME Boiler and Pressure Vessel Code, Section III, Rules for Construction of Nuclear Power Plant Components, Div. 1, Subsection NH, Class 1 Components in Elevated Temperature Service, ASME; 2004.

[6] Section I Subsection B, Design and Construction Rules for Mechanical Components of FBR Nuclear Islands, RCC-MR, 2002 Edition, AFCEN; 2002.

[7] M Cabrillat, M Mottot, C Escaravag, L Allais, B Riou, Creep-fatigue behavior of damage assessment for mod 9Cr-1Mo steel, PVP2006-ICPVT-11-93238, July 23-27, Vancouver, Canada; 2006.

[8] T McGreevy, R Jetter, DOE-ASME Generation IV materials tasks, PVP2006-ICPVT-11-93461, July 23-27, Vancouver, Canada, 2006.

[9] H-Y Lee, J-B Kim, S-H Kim, J-H Lee, "Assessment of Creep-Fatigue Crack Initiation for Welded Cylindrical Structure of Austenitic Stainless Steels," International Journal of Pressure Vessel and Piping, 83: 826-834, 2006.

[10] H-Y Lee, J-H Lee, B-H Kim, "Creep-fatigue damage for a structure with dissimilar metal welds of Mod 9Cr-1Mo and 316L stainless steel," Journal of Mechanical Science and Technology, 20(12) : 2136-2146, 2006.

[11] Ph. Metheron, S. Chapuliot, Fatigue initiation of crack under mode III and mixed mode I+III Loads in a 9Cr steel 18th int. conf. on SMIRT, Beijing, China, pp. 1896-1903, August 7-12, 2005.

[12] ASME Boiler and Pressure Vessel Code, Section II, Materials, Part D Properties, ASME, 2004.

[13] J.S. Park, "Standard Procedure of Replication for High Temperature Equipment Life Estimation," Proc. of KSME, A(24) : 2381-2386, 2000.

[14] ABAQUS Users manual, Version 6.4, H.K.S, USA; 2004.

[15] L Severud, Creep-fatigue assessment methods using elastic analysis results and adjustment, The 1989 ASEM PVP conference Honolulu, Hawaii, pp.1-8. ASME; 1989.

[16] A Aoto, R Komine, F Ueno, H Kawasaki, Y Yada, Creep-fatigue evaluation of normalized and tempered modified 9Cr 1Mo, Nuclear Engineering and Design 153: 97-110, 1994.

[17] Section I Subsection B, Technical Appendix 16, Design and Construction Rules for Mechanical Components of FBR Nuclear Islands, RCC-MR, 2002 Edition, AFCEN; 2002.

[18] H-Y Lee, J-B Kim, J-H Lee, "Evaluation of Progressive Inelastic Deformation for the Welded Structure Induced by Spatial Variation of Temperature, International Journal of Pressure Vessel and Piping, 81 (5), 433-441, 1994.

[19] H-Y Lee, J-B Kim, J-H Lee, Thermal ratcheting deformation for 316L stainless steel cylindrical structure under moving temperature distribution, International Journal of Pressure Vessel and Piping, 80, 41-48, 2003.

[20] H-Y Lee, J-B Kim, J-H Lee, J-M Lee, Thermal ratcheting behavior of a cylindrical specimen with plate-to shell junction, International Journal of Modern Physics B, 17, 797-802, 2003.

[21] H-Y Lee, J-B Kim, J-H Lee, Progressive inelastic deformation characteristics of cylindrical structure with plate-to-shell junction under moving temperature front, Korean Society of Mechanical Engineering (KSME) International Journal, 17(3), 403-411, 2003.

[22] Section I Subsection Z Technical Appendix A3, Design and Construction Rules for Mechanical Components of FBR Nuclear Islands, RCC-MR, 2002 Edition, AFCEN; 2002.